DOI 10.2478/ama-2025-0083

STRENGTH AND SUPERPLASTICITY OF AA 7075 ALUMINUM ALLOY FABRICATED BY MULTIDIRECTIONAL FORGING

Manh Hung LE*, **Manh Tien NGUYEN****, **Truong An NGUYEN****

*General Department of Military Industries and Manufacture, 100000 Ha Noi, Viet Nam
**Faculty of Mechanical Engineering, Le Quy Don Technical University, 100000 Ha Noi, Viet Nam

lemanhhungtkvcn@gmail.com, manhtiennguyen84@lqdtu.edu.vn, nguyentruongan@lqdtu.edu.vn

received 15 August 2025, revised 03 November 2025, accepted 11 November 2025

Abstract: This study explores the influence of multidirectional forging (MDF) on the mechanical strength and superplastic behavior of AA7075 aluminum alloy. The material, initially processed by hot extrusion, underwent severe plastic deformation (SPD) through MDF. Evaluations of mechanical enhancement were performed using both microhardness and tensile tests. After completing three and four MDF cycles, the alloy exhibited microhardness improvements of 48% and 60%, respectively. Corresponding increases in tensile strength were 22.45% and 40.8% relative to the untreated samples. Superplastic deformation experiments were carried out at 530 °C using strain rates of 10^{-4} s^{-1}, 10^{-3} s^{-1}, and 10^{-2} s^{-1}. The superplastic characteristics were assessed through the measurement of elongation and flow stress during tensile loading. The best performance was achieved after four MDF passes at a strain rate of 10^{-3} s^{-1}, yielding a maximum elongation of 350% and a flow stress of 9 MPa. These findings highlight the effectiveness of MDF in improving the strength and ductility of high-performance aluminum alloys while preserving their capacity for extensive plastic deformation.

Key words: AA7075 aluminum alloy, Superplasticity, multidirectional forging (MDF), severe plastic deformation (SPD), microhardness, tensile test

1. INTRODUCTION

The AA7075 aluminum alloy is extensively employed in structural and aerospace applications due to its notable strength and inherent corrosion resistance [1,2]. Despite these favorable characteristics, it is categorized among the ultra-high strength aluminum alloys, exhibiting significant resistance to both stress and deformation. This feature, while beneficial for service performance, presents considerable challenges in formability, thereby limiting its application in complex-shaped components [3,4]. To enhance the industrial applicability of AA7075, there is a growing demand for materials that exhibit both superior strength and adequate plastic deformability. In response, several innovative approaches have been explored. Among them, the integration of severe plastic deformation (SPD) techniques with superplastic deformation (SP) has emerged as a particularly promising strategy [5,6].

SPD methods induce substantial plastic strain in metallic materials, leading to the development of the UFG structures through dislocation multiplication and the formation of sub-grain boundaries [7,8]. These techniques facilitate grain refinement, thereby improving the mechanical properties of processed materials. Common SPD techniques include equal channel angular pressing (ECAP) [9,10], high-pressure torsion (HPT) [11,12], cyclic expansion-extrusion (CEE) [13,14], and multidirectional forging (MDF) [15,16]. UFG materials produced by these processes typically exhibit enhanced strength, hardness, and wear resistance. However, such materials often suffer from drawbacks like microstructural instability and reduced ductility under plastic deformation conditions [17,18].

In one notable study, Seungwon Lee et al. [19] applied the high-pressure sliding (HPS) process to improve the mechanical performance of AA7075. Post-processing, the alloy achieved a tensile strength of approximately 600 MPa with an elongation of 4%. Nevertheless, the method demands high-pressure equipment, which increases investment and operational costs. Another study by Seyed Mahmoud Ghalehbandi et al. [20] evaluated the influence of post-ECAP aging on AA7075 alloy. Their findings indicated a marked enhancement in both tensile strength and elongation, although the ECAP process is limited by tool wear and significant material loss per cycle. Among SPD methods, MDF has gained particular attention due to its operational simplicity and lower equipment cost [21-23]. Furthermore, MDF subjects materials to high hydrostatic pressure during deformation, promoting grain refinement and the formation of UFGs, which consequently enhance mechanical properties [24,25].

In parallel, superplasticity refers to the capacity of certain alloys to undergo extensive elongation under appropriate conditions of grain size, temperature, and strain rate, while subjected to minimal flow stresses [26-28]. This phenomenon typically occurs in materials with grain sizes below 15 μm. During superplastic deformation, grain growth is minimal, provided the temperature-ranging between $0.5T_m$ to $0.9T_m$ (T_m: melting point in Kelvin)-is maintained uniformly across the specimen. Moreover, the strain rate must be optimized to balance diffusion activation and grain coarsening. Superplasticity is generally observed at strain rates between 10^{-4} s^{-1} and 10^{-2} s^{-1}. SPD processes are therefore ideal for generating the UFG structures required for superplastic behavior.

Based on this background, the present study experimentally investigates the mechanical performance and superplastic response

of AA7075 alloy processed via MDF. Hot-extruded AA7075 samples were subjected to the MDF process as a form of SPD. Mechanical characterization included hardness measurements and tensile testing, while superplasticity was evaluated through tensile deformation conducted at various strain rates. Parameters such as elongation to failure and flow stress were used to assess superplastic behavior. The results aim to demonstrate the combined benefits of MDF and superplastic deformation in simultaneously achieving high strength and superior plasticity in AA7075 alloy.

2. MATERIALS AND METHODS

In this investigation, hot-extruded AA7075 aluminum alloy was selected as the experimental material. The alloy's chemical composition (in wt.%) comprises 5.35% Zn, 2.34% Mg, 1.32% Cu, 0.3% Fe, 0.05% Si, 0.024% Mn, 0.22% Cr, 0.04% Ti, with the remainder being Al. Rectangular specimens with dimensions of 17 mm × 17 mm × 25 mm (height × width × length) were precisely machined for the MDF process, as illustrated in Figure 1(a). The surface quality of the prepared samples corresponds to a roughness grade of 7, with an Ra value of 1.25 μm. A schematic representation of the MDF processing steps is depicted in Figure 1(b). Each MDF cycle consists of three deformation steps interspersed with three orthogonal rotations of the sample by 90° about the Z-, Y-, and X-axes, respectively. The deformation was applied using a YH32/100 hydraulic press with a maximum loading capacity of 100 tons. The average strain rate during the MDF process was maintained at approximately 10^{-1} s^{-1}. The die and punch were fabricated from SKD61 tool steel (JIS G4404:2015), heat-treated to achieve a hardness of 50–55 HRC.

The MDF process was conducted over one to four cycles at a constant die and sample temperature of 530 °C. The entire forming setup, including the sample and die assembly, was heated in a resistance furnace to ensure temperature uniformity during pressing. Immediately after each MDF cycle, the specimens were quenched in water to preserve the deformation-induced microstructural features.

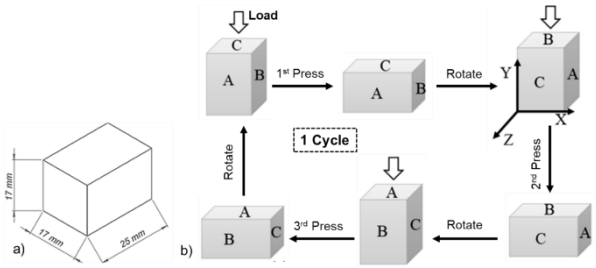

Fig. 1. Original sample (a) and MDF process diagram with 1 cycle in three sample directions (b)

Subsequent to processing, the initial and deformed microstructures were characterized and compared. Mechanical properties of both as-received and MDFed samples were assessed through Vickers microhardness measurements and uniaxial tensile testing conducted at ambient conditions. To evaluate the superplastic response, additional tensile tests were performed on the MDFed samples at 530 °C, corresponding to the forming temperature, under varying strain rates of 10^{-4} s^{-1}, 10^{-3} s^{-1}, and 10^{-2} s^{-1} [29,30]. These tests were carried out on specimens machined in accordance with ISO 6892-1:2016 specifications.

Chemical composition verification of the AA7075 alloy was conducted using a LAB LAVM11 optical emission spectrometer. Microstructural observations were carried out with an AXIOVERT-25C optical microscope. For metallographic examination, the samples were etched using an etchant composed of 95 mL distilled water, 2.5 mL HNO_3, 1.5 mL HCl, and 1.0 mL HF. Vickers microhardness was measured using a Mitutoyo hardness testing device. Tensile tests were performed on a Devotrans DVT FU/RDNN 50 kN-CKS universal testing machine equipped with continuously adjustable strain rate control. To ensure precise thermal conditions during high-temperature deformation, a Nabertherm B180 resistance furnace was employed.

3. RESULTS AND DISCUSSION

The microstructural characteristics of the as-extruded AA7075 aluminum alloy are presented in Figure 2(a). As observed, the material exhibits elongated grains with second-phase particles predominantly aligned in the direction of extrusion. This directional grain structure reflects a typical deformation-induced anisotropy that tends to reduce the alloy's mechanical efficiency, particularly in terms of ductility and strength. The anisotropic grain morphology serves as a potential initiation site for stress concentration during mechanical loading, which can impair the alloy's formability and fatigue resistance. Mechanical characterization of the as-received condition indicates a relatively low ductility, with an elongation of approximately 8% at ambient temperature, along with a mean Vickers microhardness of around 125 HV. These baseline properties underscore the need for microstructural refinement to enhance mechanical performance for advanced applications.

To investigate the influence of severe plastic deformation on microstructural evolution, the material was subjected to MDF for multiple cycles. Specimens deformed through one to four passes are designated as MDF-1, MDF-2, MDF-3, and MDF-4, respectively. Microstructural observations of both the initial and MDF-processed samples were carried out on the longitudinal–transverse (LD–TD) plane, where LD and TD correspond to the longitudinal (length) and transverse (width) directions, respectively. Figure 2(b) to Figure 2(d) illustrate the microstructures developed after each deformation stage. In the MDF-1 condition (Figure 2(b)), large and irregularly distributed precipitates are observed along grain boundaries, signaling the initial stage of microstructural reorganization. The applied compressive stress during MDF initiates grain boundary sliding and promotes the nucleation of new grains along the direction of plastic flow. At this stage, elongated grains start to fragment, and subgrains begin to form due to the accumulation of dislocations and local misorientations.

Among the grain refinement mechanisms involved, continuous dynamic recrystallization (CDRX) is considered the dominant process during MDF processing [31]. As plastic deformation progresses with additional forging cycles, shear bands intersect due to the change in loading direction, promoting the progressive subdivision of elongated grains into finer subgrains. These subgrains undergo further refinement and coalesce into equiaxed UFGs through successive recrystallization and enhanced strain hardening. The multidirectional nature of the applied deformation plays a critical role in disrupting the prior grain alignment and accelerating the transformation toward an equiaxed structure.

Notably, with each additional MDF cycle, a significant reduction in grain size is observed. For instance, in the MDF-3 sample (Figure 2(c)), the average grain size is refined to approximately 5 μm. In the

DOI 10.2478/ama-2025-0083

MDF-4 condition (Figure 2(d)), further grain fragmentation results in an average grain size of about 3 μm. This progressive microstructural refinement confirms the effectiveness of the MDF process in promoting ultrafine-grained structures within the AA7075 alloy matrix. The substantial grain refinement is expected to significantly improve the mechanical properties of the alloy, particularly its strength, hardness, and potential superplastic behavior. Therefore, the MDF technique offers a promising route for tailoring the microstructure of high-strength aluminum alloys for use in aerospace, defense, and other advanced engineering applications.

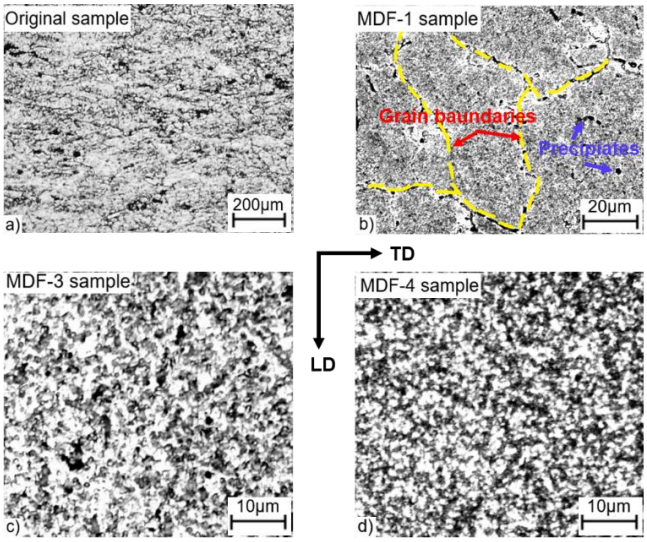

Fig. 2. Cross-sectional optical microstructure of the samples: (a) the original sample; b) the MDF-1 sample; c) the MDF-3 sample; (d) the MDF-4 sample

The distribution of microhardness across specimens subjected to MDF was systematically evaluated along both the longitudinal and transverse directions at the mid-thickness plane. The results obtained for MDF-3 and MDF-4 samples are illustrated in Figure 3(a) and Figure 3(b)), respectively. A clear non-uniformity in hardness distribution was observed throughout the samples, revealing higher microhardness values near the outer regions and relatively lower values toward the central zones. This inhomogeneous profile is primarily attributed to frictional interactions and thermal gradients that develop during the forging process. Specifically, the direct contact between the specimen and the die surfaces leads to localized cooling and elevated friction near the sample edges. These conditions enhance strain localization and promote strain hardening in those regions, thereby contributing to increased microhardness despite the slightly lower processing temperatures.

As the number of MDF passes increases, the spatial variation in microhardness becomes progressively less pronounced. This behavior indicates an improvement in strain and temperature distribution uniformity throughout the material during the later stages of deformation. For instance, in the longitudinal direction (Figure 3(a)), the disparity between maximum and minimum microhardness values was approximately 15% in MDF-3 and decreased markedly to about 4% in MDF-4. A similar trend was noted in the transverse direction (Figure 3(b)), where the variation reduced from 12% in MDF-3 to around 5% in MDF-4. These reductions in variation confirm that multiple MDF cycles facilitate a more homogeneous deformation process, both thermally and mechanically, across the entire volume of the specimen.

This observed trend aligns with the theoretical equivalent strain values, which increase substantially with each deformation cycle. Specifically, the average equivalent strain rises from approximately 0.445 after the first MDF cycle to about 1.78 following four complete cycles [16]. This enhanced strain accumulation directly correlates with the rise in microhardness and its improved distribution. Given the well-established relationship between plastic strain, dislocation density, and microhardness, the results strongly support the conclusion that severe plastic deformation via MDF contributes significantly to material hardening.

In terms of absolute values, the peak microhardness values along the longitudinal axis were recorded at 185 HV for MDF-3 and increased to 195 HV for MDF-4, corresponding to improvements of 60 HV and 70 HV, respectively, compared to the undeformed state (125 HV). In the transverse direction, slightly higher maximum hardness values were observed-185 HV for MDF-3 and up to 205 HV for MDF-4-reflecting total increases of 65 HV and 80 HV. These findings underscore the effectiveness of MDF processing in not only refining the grain structure but also enhancing the overall mechanical response of the AA7075 alloy. The substantial increase in hardness and the concurrent reduction in property gradients confirm the potential of MDF as a viable route for producing high-performance ultrafine-grained aluminum alloys with superior strength and mechanical uniformity.

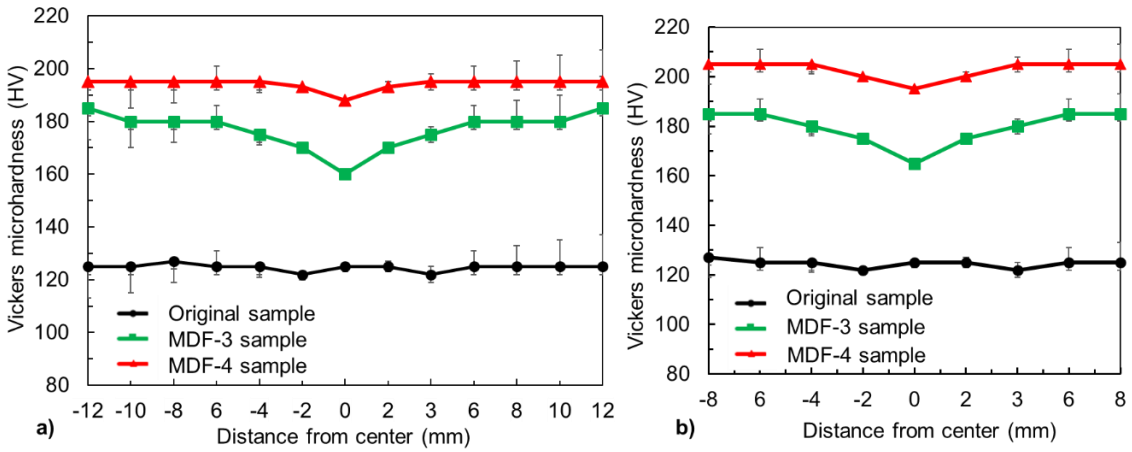

Fig. 3. Change of microhardness determined at the mid-section positions with distance from the center of the MDFed sample in the length direction (a) and width direction (b) for the MDF-3 sample and the MDF-4 sample

Figure 4 presents the engineering stress–strain curves obtained from uniaxial tensile tests conducted at room temperature for the as-received AA7075 aluminum alloy and for specimens processed through three and four passes of multidirectional forging (MDF-3 and MDF-4, respectively). The undeformed sample exhibited a tensile strength of approximately 490 MPa and a relatively low elongation of about 8%, reflecting the typical behavior of coarse-grained, hot-extruded 7xxx-series aluminum alloys. Following three cycles of MDF processing, a substantial improvement was observed: the tensile strength increased to approximately 600 MPa, accompanied by a ductility enhancement to 12%. Continued deformation with a fourth MDF cycle further elevated the tensile strength to 690 MPa and elongation to 16.5%. These results clearly demonstrate a consistent trend of simultaneous enhancement in both strength and ductility with an increasing number of MDF cycles.

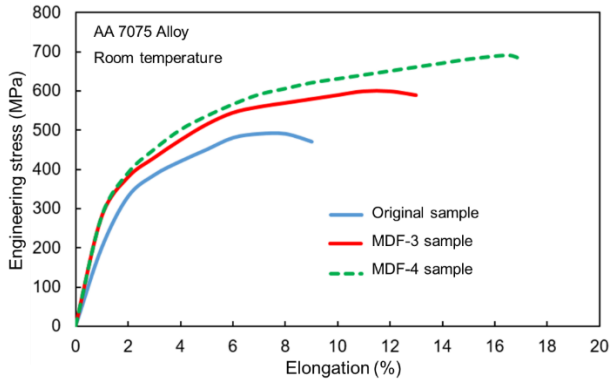

Fig. 4. Engineering stress-relative elongation curves of the original sample, the MDF-3 sample, and the MDF-4 sample

The MDF-4 specimen, in particular, showed remarkable improvement compared to the as-received material, with a tensile strength increment of 200 MPa and more than a twofold increase in elongation. Even when compared to the MDF-3 condition, the additional forging cycle resulted in a further gain of 90 MPa in strength and a 4.5% rise in ductility. These findings highlight the effectiveness of MDF in not only increasing mechanical strength, as often expected in SPD processes, but also enhancing the alloy's capacity for plastic deformation-a result that defies the conventional strength-ductility trade-off.

The origin of this mechanical performance improvement lies primarily in the extensive grain refinement introduced by the MDF technique. As the number of forging passes increases, the average grain size is significantly reduced, leading to the formation of a dense network of grain boundaries. The increased grain boundary area plays a vital role in governing mechanical behavior, as it acts as an effective barrier to dislocation motion, thereby enhancing strength. Simultaneously, grain boundaries also serve as active sites for alternative deformation mechanisms, including grain boundary sliding and grain rotation, which contribute to enhanced ductility in UFG materials [32].

Additionally, the formation of a UFG structure modifies the material's internal lattice arrangement. The thin and highly dense interfaces between grains lead to improved atomic packing, stronger interatomic bonds, and a lower density of lattice defects. These structural characteristics help suppress the formation of microcracks during tensile deformation, thus extending the material's ductility and delaying failure [6]. In polycrystalline metals, deformation is typically accommodated through both intragranular slip and grain boundary activities. In UFG materials produced by MDF, the high grain boundary density facilitates distributed plasticity under applied load, allowing for more uniform strain distribution and enhancing the alloy's overall formability.

In summary, the stress-strain behavior of AA7075 subjected to MDF confirms that repeated multidirectional deformation effectively tailors the microstructure, resulting in a well-balanced combination of high strength and enhanced ductility. This positions MDF as a promising processing technique for advanced applications requiring lightweight, high-performance structural components.

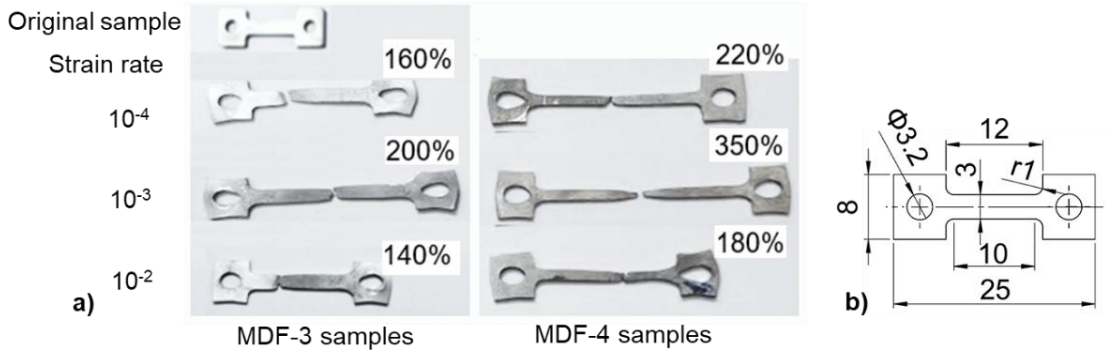

Fig. 5. Shape changes in the tensile samples of AA7075 alloy fabricated by MDF-3 sample and MDF-4 sample under the superplastic deformation conditions (a); and dimension of the tensile samples (b)

This explanation also supports the observed trend in which relative elongation increases with decreasing average grain size in MDF-processed samples. As presented in Figure 5 and , the tensile behavior of AA7075 alloy subjected to 3 and 4 cycles of MDF under SPD conditions reveals a clear distinction. When tested at identical temperatures and strain rates, the specimens processed by four MDF passes (MDF-4) consistently exhibit higher relative elongation than those processed by three passes (MDF-3). Specifically, the increase in elongation reaches 37.5%, 75%, and 28.6% at strain rates of 10^{-4} s^{-1}, 10^{-3} s^{-1}, and 10^{-2} s^{-1}, respectively. These enhancements are strongly associated with the reduced grain size of the MDFed specimens. From a theoretical perspective, grain boundary sliding (GBS) is considered the dominant mechanism governing superplastic deformation. GBS facilitates large strain accommodation, retention of equiaxed grain structures, grain rotation, and texture evolution. Experimental evidence of GBS includes the

DOI 10.2478/ama-2025-0083

relative displacement of adjacent grains along their boundaries, ultimately leading to the replacement of neighboring grains-a phenomenon characteristic of superplasticity that does not occur during conventional plastic deformation [33].

Under superplastic deformation conditions, it is well established that individual grains exhibit minimal morphological changes. Even when some grains appear slightly elongated, the extent of their elongation remains significantly lower than the overall relative elongation of the specimen. The near-constant grain shape observed within the superplastic strain rate regime implies that substantial deformation arises primarily from the relative displacement between neighboring grains, leading to enhanced grain density along the tensile direction. This behavior results in a high degree of elongation. According to the GBS mechanism, deformation is predominantly localized at grain boundaries. Hence, a reduction in grain size increases the total grain boundary area, which facilitates larger relative elongation during tensile loading [34].

Tab.1. Tensile test results of the MDF-processed samples at different strain rates

Samples	Elongations (%)		
	Strain rate 10^{-4} (s^{-1})	Strain rate 10^{-3} (s^{-1})	Strain rate 10^{-2} (s^{-1})
MDF-3	160	200	140
MDF-4	220	350	180

The presence of the UFG in the microstructure of MDF-processed samples confirms the manifestation of superplasticity in the AA7075 alloy, as evidenced by tensile tests conducted under superplastic conditions. All tensile specimens displayed elongations exceeding 140%, accompanied by relatively low flow stress levels. A comparative analysis of the tensile behavior of samples extracted from MDF-3 and MDF-4 specimens (as shown in Figure 5 and Figure 6) reveals a clear dependence on strain rate. As the strain rate increases from 10^{-4} s^{-1} to 10^{-3} s^{-1}, the relative elongation improves. However, a further increase in strain rate to 10^{-2} s^{-1} results in a decline in elongation (Figure 6 (c)).

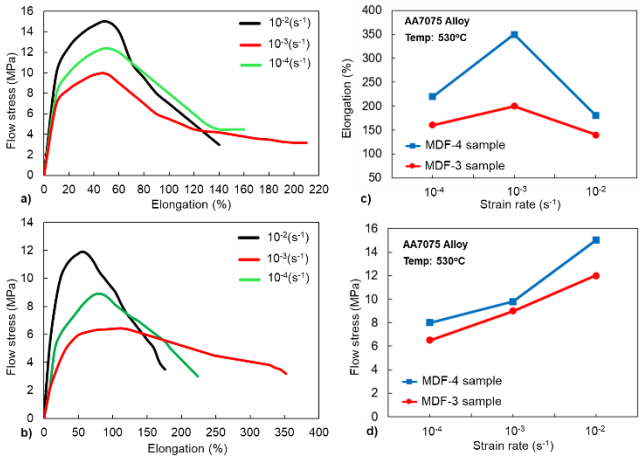

Fig. 6. The flow stress - relative elongation curves at 530 °C for the MDF-3 sample (a), the MDF-4 sample (b) and the elongation and the flow stress of the MDFed (c,d) with different strain rates

For MDF-4 specimens, the maximum elongations recorded at strain rates of 10^{-4} s^{-1}, 10^{-3} s^{-1}, and 10^{-2} s^{-1} were 220%, 350%, and 180%, respectively. In contrast, the MDF-3 samples exhibited elongations of 160%, 200%, and 140% at the corresponding strain rates. These findings underscore the strong influence of strain rate on the superplastic response of UFG AA7075 alloy fabricated via MDF. At strain rates below 10^{-4} s^{-1}, excessive grain growth occurs due to prolonged dynamic recrystallization (DRX) times, which in turn induces premature necking and limits elongation [35,36]. Conversely, at strain rates exceeding 10^{-2} s^{-1}, the deformation rate surpasses the capacity for diffusion-assisted mechanisms to develop favorable sliding interfaces, leading to increased flow stress and reduced ductility [37,38]. In summary, among the tested strain rates, the optimal superplastic response was observed at 10^{-3} s^{-1}. The maximum relative elongations achieved at this rate were 200% for MDF-3 samples and 350% for MDF-4 samples.

Additionally, Figure 6(d) highlights the combined effect of grain size and superplastic strain rate on the maximum flow stress observed during tensile testing. The MDF-4 specimens, which possess a finer grain structure, consistently exhibit lower flow stress values than the MDF-3 specimens across all investigated strain rates. Specifically, for MDF-4 samples, the flow stress values at strain rates of 10^{-4} s^{-1}, 10^{-3} s^{-1}, and 10^{-2} s^{-1} are 6.5 MPa, 9 MPa, and 12 MPa, respectively. In comparison, the corresponding values for MDF-3 samples are higher, at 8 MPa, 9.8 MPa, and 15 MPa, respectively.

These differences can be attributed to the initial grain size of the samples. The UFG microstructure of MDF-4 samples results in a greater grain boundary area, which enhances grain boundary sliding and promotes more uniform plastic flow, thereby lowering the required flow stress. Furthermore, an increasing trend in flow stress with increasing strain rate is clearly observed. At lower strain rates and elevated temperatures, sufficient time is available for atomic diffusion, which facilitates the formation of favorable slip planes and reduces flow resistance. In contrast, higher strain rates limit the diffusion processes, leading to an increase in flow stress during deformation [39].

4. CONCLUSION

In this study, an experimental approach was employed to examine the evolution of mechanical strength and superplastic behavior of AA7075 aluminum alloy subjected to the MDF technique. The primary outcomes of the investigation are summarized as follows:

1. The MDF method demonstrated considerable effectiveness in refining the grain structure and generating UFG microstructures. The process was performed at an elevated temperature of 530 °C over multiple deformation cycles. The resulting average grain sizes were approximately 5 μm and 3 μm for the MDF-3 and MDF-4 specimens, respectively. These refined grain sizes fulfill the microstructural prerequisites for enabling superplastic deformation.

2. Mechanical performance of the AA7075 alloy was substantially enhanced following MDF processing. In particular, microhardness measurements revealed increases of 48% and 60% for the MDF-3 and MDF-4 samples, respectively, in comparison to the undeformed condition. Additionally, tensile test results indicated concurrent improvements in strength and ductility. For the MDF-3 sample, the tensile strength and total elongation were recorded at 600 MPa and 12%, respectively. In the case of the MDF-4 specimen, tensile strength reached 690 MPa, accompanied by an elongation of 16.5%. These values correspond to an improvement of 200 MPa in tensile strength and an 8.5% increase in ductility compared to the unprocessed alloy.

3. Specimens processed through three and four MDF cycles exhibited pronounced superplastic behavior when tested at 530 °C across a range of strain rates (10^{-4} s^{-1}, 10^{-3} s^{-1}, and 10^{-2} s^{-1}). All tested samples demonstrated elongation-to-failure exceeding 140%, coupled with low flow stress levels. The optimal superplastic performance was observed in the MDF-4 sample at a strain rate of 10^{-3} s^{-1}, yielding a maximum elongation of 350% and a corresponding flow stress of only 9 MPa.

REFERENCES

1. Zhou B, Liu B, Zhang SG. The advancement of 7XXX series aluminum alloys for aircraft structures: a review. Metals. 2021;11(5): 718-747. https://doi.org/10.3390/met11050718
2. Miller WS, Zhuang L, Bottema J, Wittebrood AJ, De Smet P, Haszler A, et al. Recent development in aluminium alloys for the automotive industry. Mater Sci Eng A. 2000;280(1): 37-49. https://doi.org/10.1016/S0921-5093(99)00653-X
3. Georgantzia E, Gkantou M, Kamaris GS. Aluminium alloys as structural material: A review of research. Eng Struct. 2021;227: 111372. https://doi.org/10.1016/j.engstruct.2020.111372
4. Dorward RC, Pritchett TR. Advanced aluminium alloys for aircraft and aerospace applications. Mater Des. 1988;9(2): 63-69. https://doi.org/10.1016/0261-3069(88)90076-3
5. Nieh TG, Wadsworth J, Sherby OD. Superplasticity in metals and ceramics. New York: Cambridge University Press; 1997.
6. Kawasaki M, Langdon TG. Developing superplasticity in ultrafine-grained metals. Acta Phys Pol A. 2015;128(4): 470-478. https://doi.org/10.12693/APhysPolA.128.470
7. Furukawa M, Horita Z, Nemoto M, Langdon TG. Review: processing of metals by equal-channel angular pressing. J Mater Sci. 2001;36: 2835-2843. https://doi.org/10.1023/A:1017932417043
8. Zrnik J, Dobatkin SV, Mamuzi I. Processing of metals by severe plastic deformation (SPD) – Structure and mechanical properties respond. Metalurgija. 2008;47(3): 211-216.
9. Horita Z, Fujinami T, Nemoto M, Langdon TG. Equal-channel angular pressing of commercial aluminum alloys: Grain refinement, thermal stability and tensile properties. Metall Mater Trans A. 2000;31(3): 691-701. https://doi.org/10.1007/s11661-000-0011-8
10. Kapoor R, Chakravartty JK. Deformation behavior of an ultrafine-grained Al-Mg alloy produced by equal-channel angular pressing. Acta Mater. 2007;55: 5408-5418. https://doi.org/10.1016/j.actamat.2007.05.049
11. Zhilyaev AP, Langdon TG. Using high-pressure torsion for metal processing: Fundamentals and applications. Prog Mater Sci. 2008;53(6): 893-979. https://doi.org/10.1016/j.pmatsci.2008.03.002.
12. Gunderov D, Stotskiy A, Lebedev Y, Mukaeva V. Influence of HPT and accumulative high-pressure torsion on the structure and HV of a zirconium alloy. Metals. 2021;11(4): 573. https://doi.org/10.3390/met11040573
13. Do Xuan Truong, Nguyen Manh Tien, Nguyen Manh Hung, Nguyen Truong An. Effect of the cyclic expansion-extrusion process on mechanical properties and the grain refinement of AA6061 aluminum alloy. J Military Sci Technol. 2023;87: 100-107. https://doi.org/10.54939/1859-1043.j.mst.87.2023.100-107
14. Fan H, Yan Z, Zhang Z, Wang Q. Effects of cyclic expansion-extrusion with an asymmetrical extrusion cavity (CEE-AEC) on the microstructure and texture evolution of Mg-13Gd-4Y-2Zn-0.5Zr alloys. Mater Technol. 2020;54(4): 495-501. https://doi.org/10.17222/mit.2019.251
15. Nguyen MT, Le VT, Le MH, Nguyen TA. Superplastic properties in a Ti5Al3Mo1.5V titanium alloy processed by multidirectional forging process. Mater Lett. 2022;307: 131004. https://doi.org/10.1016/j.matlet.2021.131004
16. G. A. Manjunath, S. Shivakumar, R. Fernandez, R. Nikhil, and P. C. Sharath. A review on effect of multi-directional forging/multi-axial forging on mechanical and microstructural properties of aluminum alloy. Mater. Today: Proc. 2021;47(9): 2565-2569. https://doi.org/10.1016/j.matpr.2021.05.056
17. Valiev RZ, Islamgaliev RK, Alexandrov IV. Bulk nanostructured materials from severe plastic deformation. Prog Mater Sci. 2000;45(2): 103-189. https://doi.org/10.1016/S0079-6425(99)00007-9.
18. Yan L, Li Q, Chen X. Research of severe plastic deformation on magnesium alloys. Trans Mater Heat Treat. 2018;39(11): 1-9. https://doi.org/10.13289/j.issn.1009-6264.2018-0308
19. Lee S, Tazoe K, Mohamed IF, Horita Z. Strengthening of AA7075 alloy by processing with high-pressure sliding (HPS) and subsequent aging. Mater Sci Eng A. 2015;628: 56-61. https://doi.org/10.1016/j.msea.2015.01.026
20. Ghalehbandi SM, Fallahi A, Hosseini-Toudeshky H. Influence of aging on mechanical properties of equal channel angular pressed aluminum alloy 7075. Proc Inst Mech Eng B. 2015;231(10): 1803-1811. https://doi.org/10.1177/0954405415612370
21. Xu X, Zhang Q, Hu N, Huang Y, Langdon TG. Using an Al-Cu binary alloy to compare processing by multi-axial compression and high-pressure torsion. Mater Sci Eng A. 2013;588: 280-287. https://doi.org/10.1016/j.msea.2013.09.001
22. G. A. Manjunath, S. Shivakumar, S. P. Avadhani, and P. C. Sharath. Investigation of mechanical properties and microstructural behavior of 7050 aluminium alloy by multi directional forging technique. Mater. Today: Proc. 2020;27(2): 1147-1151. https://doi.org/10.1016/j.matpr.2020.02.001
23. Ghanbari BF, Arabi H, Abbasi SM, Boutorabi MA. Manufacturing of nanostructured Ti-6Al-4V alloy via closed-die isothermal multi-axial-temperature forging: Microstructure and mechanical properties. Int J Adv Manuf Technol. 2016;87: 755-763. https://doi.org/10.1007/s00170-016-8343-8
24. Wei C, Lei Z, Du S, Chen R, Yin Y, Niu C, et al. Microstructures and mechanical properties of Al-Zn-Mg-Cu alloys under multi-directional severe strain and aging. Materials. 2023;16(12): 4441. https://doi.org/10.3390/ma16124441
25. Manjunath GA, Shivakumar S, Fernandez R, Nikhil R, Sharath PC. A review on effect of multi-directional forging/multi-axial forging on mechanical and microstructural properties of aluminum alloy. Mater Today Proc. 2021;47(10): 2565-2569. https://doi.org/10.1016/j.matpr.2021.05.056
26. Kawasaki M, Langdon TG. Superplasticity in ultrafine-grained materials. Rev Adv Mater Sci. 2018;54(1): 46-55. https://doi.org/10.1515/rams-2018-0019
27. Nguyen MT. Experimental determination of process parameters for superplastic forming from AA7075 aluminum alloy. Suranaree J Sci Technol. 2022;29(5): 0101631.
28. Prasad VJ, Mohanarao N, Kamaluddin S, Bhattacharya SS. Development of superplasticity in an Al-Mg alloy through severe plastic deformation. Int J Adv Manuf Technol. 2018;94: 2973-2979. https://doi.org/10.1007/s00170-017-1060-0
29. Giuliano G. Superplastic forming of advanced metallic materials. Cambridge: Woodhead Publishing; 2011.
30. Xu GF, Cao XW, Zhang T, Li Q, Wang Z, Wang W, et al. Achieving high strain rate superplasticity of an Al-Mg-Sc-Zr alloy by a new asymmetrical rolling technology. Mater Sci Eng A. 2016;672: 98-107. https://doi.org/10.1016/j.msea.2016.06.070
31. Zhang S, Hu W, Berghammer R, Gottstein G. Microstructure evolution and deformation behavior of ultrafine-grained Al-Zn-Mg alloys with fine η' precipitates. Acta Mater. 2010;58(20): 6695-6705. https://doi.org/10.1016/j.actamat.2010.08.034
32. Azushima A, Kopp R, Korhonen A, Yang DY, Micari F, Lahoti GD, et al. Severe plastic deformation (SPD) processes for metals. CIRP Ann. 2008;57(2): 716-735. https://doi.org/10.1016/j.cirp.2008.09.005
33. Asgharzadeh H, McQueen HJ. Grain growth and stabilisation of nanostructured aluminium at high temperatures: Review. Mater Sci Technol. 2015;31(9): 1016-1034. https://doi.org/10.1179/1743284714Y.0000000706
34. Liew KM, Tan MJ, Tan H. Analysis of grain growth during superplastic deformation. Mech Adv Mater Struct. 2007;14(7): 541-547. https://doi.org/10.1080/15376490701586023

DOI 10.2478/ama-2025-0083

35. Nieh TG, Hsiung LM, Wadsworth J, Kaibyshev R. High strain rate superplasticity in a continuously recrystallized Al-6%Mg-0.3%Sc alloy. Acta Mater. 1998;46(8): 2789-2800. https://doi.org/10.1016/S1359-6454(97)00452-7
36. Li M, Pan Q, Shi Y, Sun X, Xiang H. High strain rate superplasticity in an Al-Mg-Sc-Zr alloy processed via simple rolling. Mater Sci Eng A. 2017;687: 298-305. https://doi.org/10.1016/j.msea.2017.01.091
37. Wang XG, Li QS, Wu RR, Zhang XY, Ma L. A review on superplastic formation behavior of Al alloys. Adv Mater Sci Eng. 2018;2018: 1-17. https://doi.org/10.1155/2018/7606140
38. Abo-Elkhier M, Soliman MS. Superplastic characteristics of fine-grained 7475 aluminum alloy. J Mater Eng Perform. 2006;15(1): 76-80. https://doi.org/10.1361/105994906X83394
39. Ye L, Zhang X, Zheng D, Liu S, Tang J. Superplastic behavior of an Al-Mg-Li alloy. J Alloys Compd. 2009;487(1-2): 109-115. https://doi.org/10.1016/j.jallcom.2009.07.148

The authors would like to express their sincere gratitude to the Le Quy Don Technical University for providing laboratory facilities and technical support throughout this research.

Manh Hung Le: https://orcid.org/0009-0008-1778-2092
Manh Tien Nguyen: https://orcid.org/0000-0003-2525-2645
Truong An Nguyen: https://orcid.org/0000-0003-2506-3086